Available online at www.sciencedirect.com

ScienceDirect

Energy Procedia 120 (2017) 673–680

Energy Procedia

www.elsevier.com/locate/procedia

INFUB - 11th European Conference on Industrial Furnaces and Boilers, INFUB-11

Numerical Studies of Premixed and Diffusion Meso/Micro-Scale Flames

A. Cova[a], P. R. Resende[b], A. Cuoci[c], M. Ayoobi[d], A. M. Afonso[a,*] and C. T. Pinho[a]

[a]*CEFT, Department of Mechanical Engineering, University of Porto, Portugal*
[b]*São Paulo State University (Unesp), Institute of Science and Technology, Sorocaba, Brazil*
[c] *Dipartimento di Chimica, Materiali ed Ingegneria Chimica "G. Natta", Politecnico di Milano, Italy*
[d]*Div. of Engineering Technology, College of Engineering, Wayne State Univ., Detroit, Michigan, USA*

Abstract

This work reports a numerical investigation of premixed and diffusion meso/micro-scale flames, with homogeneous reactions, for two different cases involving CH_4/*air* premixed dynamics flames and co-flow diffusion flame with H_2/N_2 mixture. In the first case, the numerical predictions are able to capture the flame characteristics behaviour for different fuel equivalent ratio and geometries, showing the accuracy of the reactions model, which uses a very detailed kinetics. In the second case, the analysis concerns the effect of a porous bluff body in pollutants emissions, especially the NO_x formation, at meso scale, considering different porous temperatures and geometrical configurations.

© 2017 The Authors. Published by Elsevier Ltd.
Peer-review under responsibility of the organizing committee of INFUB-11

Keywords: Micro-flames, diffusion; dynamics flames; porous bluff body; numerical simulation

1. Introduction

The increasing demand on combustion based micro-power generation systems, created a great opportunity to develop portable power devices, to be applied on micro unmanned aerial vehicles, micro-satellite thrusters, or micro chemical reactors and sensors [1]. However, combustion at such small scales presents several practical limitations in

* Corresponding author. Tel.:+351 220413508.
E-mail address: aafonso@fe.up.pt

1876-6102 © 2017 The Authors. Published by Elsevier Ltd.
Peer-review under responsibility of the organizing committee of INFUB-11
10.1016/j.egypro.2017.07.181

design and performance, because of the small residence time of the reactant mixture in the micro chamber, and the high external heat losses, limiting the presence of a stable flame. For this reason, the micro combustion phenomenon is currently being subject to extensive numerical and experimental research [1].

The development of better numerical models allowed gathering detailed information of the flame structure, especially to determine the range of operation conditions and new geometry configurations to obtain a stable flame, using different types of fuels. Aikun et al. [2], simulated the combustion of a hydrogen/air mixture in a 3D rectangular micro-channel, using a commercial CFD program, and analysed the effect in the flame temperature and length, when varying the inlet velocity, channel height and wall material. The temperature fields clearly showed the preheating, combustion and cooling region, where the mixture ignites and anchors near the entrance in a cone-shaped structure. The combustion remained stable and persistent for a wide velocity range, and even in the limit cases the extinction phenomena did not occur. Li et al. [3], also conducted numerical simulations for premixed hydrogen/air flames, in cylindrical and parallel plates micro-channels, and highlighted the importance of axial heat conduction to preheat the unburned mixture. They verified the influence of axial heat conduction in widening the flame stability, but also noticed that for low inlet velocities, where there is practically no contact between the wall and the unburned mixture, the axial conduction practically does not influence the flame.

To minimize the external heat losses, studies had been performed to take advantage of the heat recirculation. Chen and Ronney [4], numerically investigated the dimensionless parameters to characterized the scale effects on heat-recirculating combustors in a three-dimensional (3D) propane Swiss roll combustor. They conclude that four dimensionless parameters (Reynolds number, heat loss coefficient, Damkohler number and radiative transfer number) were sufficient to characterize the combustor performance, and establishing the extinction limits due to both heat losses and finite residence time. They also verified that at low Reynolds number (*Re*) smaller combustors had lower lean extinction limits in comparison with larger combustors, due to lower heat loss and internal wall-to-wall radiation effects; however at high Re, larger combustors proved to be better because of the longer residence time relative to chemical reaction time. Comparison with linear combustors showed, that this type of combustor presented better performance at low Re, as theoretically expected.

Li et al. [5] undertook an experimental study to analyse the possibility of extending flame stability limits of premixed *hydrogen*/*air* in a 1 mm planar micro-combustor, since this aspect is very important to its design and operation. It was found that, when the combustor is filled with a porous medium, it widens the flame stability limits, especially for the flashback critical conditions. It must be stressed that, inserting a porous medium in a combustion chamber reduces the flame temperature, and consequently reduces pollutants emissions, such as *NO* and *CO*.

In this work, it is presented a numerical study on premixed and diffusion meso/micro-scale flames, using a numerical framework for the numerical modelling of laminar flows with homogeneous reactions (laminarSMOKE). This code, developed by Cuoci et al. [6], uses very detailed kinetics to model the reactions and will be presented in section 2. The results of both test cases studied, are shown in section 3, where in the investigations for CH_4/*air* premixed flames on narrow 2D micro-channels, it was studied the transient dynamics of symmetric and asymmetric oscillating flames, as detailed by Ayoobi [7]. The effect of the premixed equivalence ratios and micro-channel heights were evaluated, and results clearly showed that symmetric flame behaviour is only observed in the narrower micro-channel. For higher micro-channel height, the ignition was followed by asymmetric limit cycles behaviour. The effect of inserting a porous bluff body (PBB) within a meso-combustion chamber was also considered. The co-flow diffusion flame was obtained with a H_2/N_2 mixture, and the pollutants emissions were analysed for different PBB temperatures and geometrical configurations. It was observed that the decrease of the temperature at the PBB surface also decreased the NO_x formation. Furthermore, reducing the size of the PBB media results in higher flow velocities and therefore lower residence times, leading to lower NO_x formation.

2. Numerical simulation

The numerical model used to simulate the test cases present in this work, is described by the conservation equations for continuous, multicomponent, compressible, thermally-perfect mixture of gases, and considered as Newtonian fluids. The conservation equations of total mass, mixture momentum, individual species mass fractions and mixture energy, are:

$$\frac{\partial \rho}{\partial t} + \nabla(\rho \mathbf{v}) = 0 \tag{1}$$

$$\frac{\partial}{\partial t}(\rho \mathbf{v}) + \nabla(\rho \mathbf{v}\mathbf{v} + p\mathbf{I}) = \nabla \tau + \rho \mathbf{g} \tag{2}$$

$$\frac{\partial}{\partial t}(\rho Y_k) + \nabla(\rho Y_k \mathbf{v}) = \nabla(\rho Y_k \mathbf{V}_k) + \dot{\Omega}_k \qquad k = 1,...,NC \tag{3}$$

$$\rho C_p \frac{\partial T}{\partial t} + \rho C_p \mathbf{v} \nabla T = -\nabla \mathbf{q} - \rho \sum_{k=1}^{NC} C_{p,k} Y_k \mathbf{V}_k - \sum_{k=1}^{NC} h_k \dot{\Omega}_k \tag{4}$$

where t is the time, ρ is the mixture density, p the pressure, v the mixture velocity vector, τ the fluid stress tensor, g the acceleration vector due to gravity, Y_k the mass fraction of species k, V_k is the diffusion velocity of species k, $\dot{\Omega}_k$ the formation rate of species k, T the temperature, C_p and C_p, k are the specific heat at constant pressure of the mixture and of the individual species k, respectively, q the heat flux vector and h_k the individual species enthalpy.

The density of the mixture is calculated through the ideal gas equation of state, while the heat flux vector, which includes conduction and radiation, is calculated as following:

$$\mathbf{q} = -\lambda \nabla T - 4\sigma a_P \left(T^4 - T_{env}^4\right) \tag{5}$$

where λ is the mixture thermal conductivity, T_{env} is the environment temperature and σ is the Stefan-Boltzmann constant. The Planck mean absorption coefficient, a_P, is estimated according to RADCAL software [8]. The radiative heat transfer was modelled by assuming the optically thin radiation hypothesis, in which self-absorption of radiation is neglected. Only the following significant radiating species, H_2O, CO, CO_2 and CH_4, were taken into account. The diffusion velocities of species k are calculated, considering both Fick's law and thermal diffusion:

$$\mathbf{V}_k = -\frac{D_k}{Y_k} \nabla Y_k - \frac{D_k \Theta_k}{X_k} \frac{1}{T} \nabla T \tag{6}$$

where X_k is the mole fraction and Θ_k the thermal diffusion ratio of species k and D_k is the individual-species mixture-averaged diffusion coefficient, which is related to the binary diffusion coefficients Γ_{jk} through the expression:

$$D_k = (1 - Y_k) \Big/ \sum_{j=1, j \neq k}^{NC} \frac{X_k}{\Gamma_{jk}} \tag{7}$$

The approach proposed by Coffee and Heimerl [9] was adopted here to enforce the mass conservation, which consists of replacing V_k in Equations (3) and (4), for a correction diffusion velocity, $\mathbf{V}_k^C$, defined as

$$\mathbf{V}_k^C = \mathbf{V}_k - \sum_{k=1}^{NC} Y_k \mathbf{V}_k \tag{8}$$

where the second term of the right-side of the equation is a constant corrector factor that is species-independent, although varies in space and time, and it is used to satisfy the mass conservation.

The equations described before are solved by the laminarSMOKE code [6], and for the combustion kinetics two different detailed mechanisms are considered, consisting of 84 species and 1698 reactions for the methane flame, and consisting of 32 species and 173 reactions for the hydrogen flame. The detailed kinetic mechanisms were developed by CRECK Modelling Group, and validated in [10]. In both cases, the conduction heat transfer trough the wall is

excluded for simplicity, reducing the computational effort due to the absence of gas solid thermal interaction. All simulations start with an internal field composed only by air at 300 K and ambient pressure. The remaining boundary conditions (BC) and geometry configuration will be described next for each case.

2.1. CH_4/air premixed dynamics flames

The burner is considered as non-slip and consisted in a 2D channel with a length of 80 mm and two different heights, 2 mm and 5 mm, using an equispaced grid with a resolution of 15 by 350 for the 2 mm channel height, and a 27 by 350 grid for the 5 mm channel height.

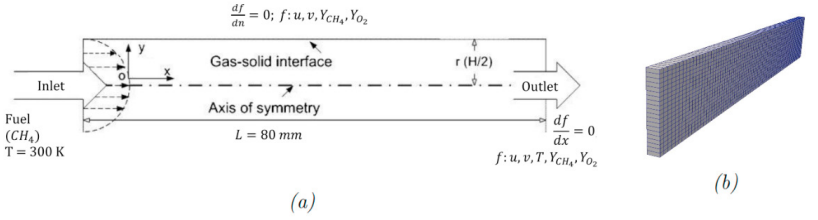

Fig. 1. (a) Schematic illustration of computational domain coupled with boundary conditions, (b) computational mesh, of CH_4 premixed flames on a narrow 2D channel.

The boundary and initial conditions as well as a computational mesh for one of the tests, are represented in Fig. 1. For the inlet, two different equivalence ratios for each simulated channel height are used for the premixed CH_4/*air*, 0.53 and 0.7, composing four different tests. The inlet velocity profile is always assumed fully developed with a mean velocity of 0.4 m/s. To simulate the effect of the wall temperature a linear temperature ramp profile is imposed on both sides: at the inlet, the wall temperature is set to 300 K, increasing linearly until 1900 K at the outlet, resulting in a gradually higher heating of the incoming unburned mixture.

2.2. Co-flow diffusion flame with H_2/N_2 mixture

Similarly to the previous case, the geometry of the burner is a 2D planar combustion chamber, with and without a porous media within the burner at micro and meso-scale. Fig. 2 (a) shows a cross-sectional view of the computational domain in which steady state combustion takes place using H_2 and N_2 fuel (0.5 molar fraction each), at ambient temperature and pressure, fed with a full developed profile with a mean velocity of 25 cm/s, surrounded by an air-co flow quadrangular annulus. The dimension of the nozzle is 8 mm long and 9 mm high, with a 1 mm width.

Fourteen different tests were simulated, combining three parameters variations: (I) the location and configuration of the porous media inside of the meso-scale combustor, (II) the height of the combustor chamber and (III) the porous surface temperature:

(I) Three different configurations were used and can be identified by: test (a) a porous media placed in the middle of the combustion chamber 30 mm distanced from the top and bottom walls, whose computational mesh is represented in Fig. 2 (b); test (b) a porous media placed in the middle of the combustion chamber confined between the top and bottom walls, whose mesh in shown in Fig. 3 (a); and test (c) a compressed porous media placed in the middle of the combustion chamber confined between the top and bottom walls, 8 mm downstream of the nozzle exit, whose mesh in shown in Fig. 3 (b).

(II) The initial dimensions of the combustor chamber were defined as 150 mm long by 95 mm high for test (a), and in the second phase the height was reduced to 35mm for the tests (b) and (c), keeping the same width of 1 mm.

(III) For each geometry, different thermal boundary conditions were employed to the porous surfaces: (0) no porous media inserted in the combustor; (1) adiabatic surface; (2) surface temperature of 1000 K; (3) surface temperature of 1250 K; (4) surface temperature of 1500 K.

The porous surfaces were set as walls and a zero gradient for the boundary conditions was imposed for all the previous parameters, excepting for the thermal BC. A non-slip BC is assumed for the porous surfaces and nozzle, whereas the combustor walls were assumed slippery. Since the flame would be ignited right after the nozzle when contacting with the O_2, it was imposed a finer refinement of the grid in this region as well as in the area involving the porous media.

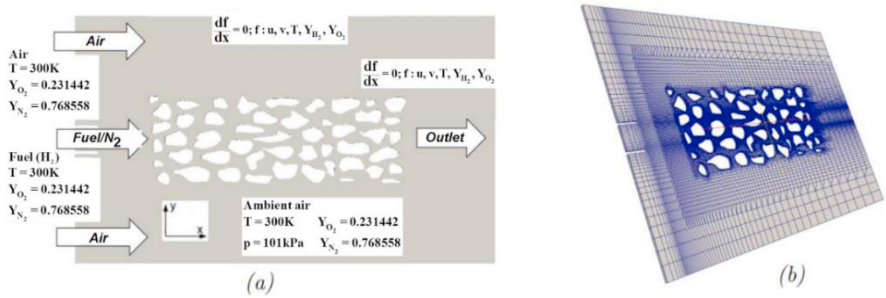

Fig. 2. (a) schematic illustration of computational domain coupled with boundary conditions, (b) computational mesh, of H2/N2 co-flow flames with a porous media inserted within the combustion chamber.

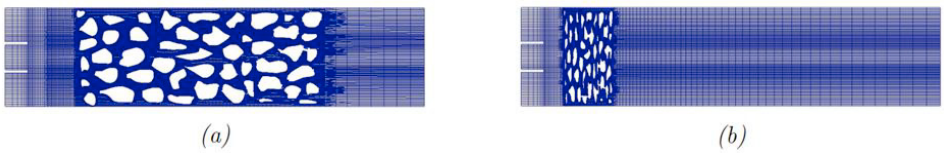

Fig. 3. Computational meshes applied for the different configurations test: (a) test (b) and (b) test (c).

All presented cases are organised in Table 1. There is no (c.0) case since it is the same as (b.0).

Table 1. Operating conditions for fourteen test cases.

Case	Porous thermal BC	Combustor dimension (length × height) [mm × mm]
(a.0)	Without porous	150 × 95
(a.1)	Adiabatic	150 × 95
(a.2)	T=1000 K	150 × 95
(a.3)	T=1250 K	150 × 95
(a.4)	T=1500 K	150 × 95
(b.0)	Without porous	150 × 35
(b.1)	Adiabatic	150 × 35
(b.2)	T=1000 K	150 × 35
(b.3)	T=1250 K	150 × 35
(b.4)	T=1500 K	150 × 35
(c.1)	Adiabatic	150 × 35
(c.2)	T=1000 K	150 × 35
(c.3)	T=1250 K	150 × 35
(c.4)	T=1500 K	150 × 35

3. Results and discussion

3.1. CH_4/air premixed dynamics flames

For the validation of the numerical code the predictions of flame dynamics in a narrow 2D channel using CH_4/*air* premixed fuel, are compared with the numerical results presented by Ayoobi [7], for several conditions. The initial

tests were performed considered the smaller combustor chamber with 2 mm of height for an equivalent ratio of ϕ=0.53 and ϕ=0.70. In Fig. 4 (a) and (b), the total heat release is shown as a function of time, and illustrates the formation of stationary and symmetric flames for both equivalence ratios. In both cases, the maximum deviation error of the total heat release for the steady-state situation is about 4%, when compared with Ayoobi [7].

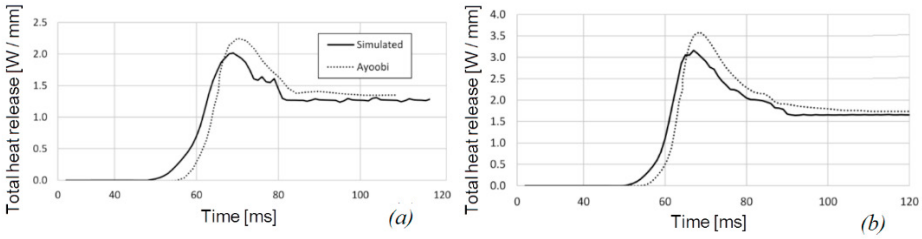

Fig. 4. Total heat release with time in a 2 by 80 mm-channel: (a) ϕ = 0.53 and (b) ϕ = 0.70. Ayoobi curve from [7].

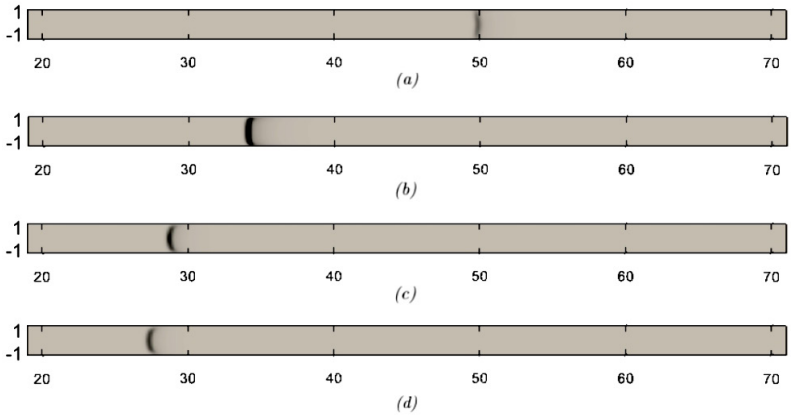

Fig. 5. Heat release fields during ignition and flame stabilization in a 2 by 80 mm-channel for ϕ = 0.7 at: a) 60 ms, b) 70 ms, c) 80 ms, d) 90 ms. A symmetric flame stabilizes after initial behaviour. The field maps are scaled from zero (grey) to 3 W/mm^3 (black).

The unburned mixture is gradually more heated up, as the wall temperature also rises along the channel, and further downstream, when gases temperatures are sufficiently high, the mixtures auto-ignite, Fig. 5.As expected, in the leaner case (ϕ = 0.53), the stationary flame anchors more downstream, in the hotter region, compared with the richer case (ϕ = 0.7), as it releases less chemical energy, even though both cases have equal inlet velocities.

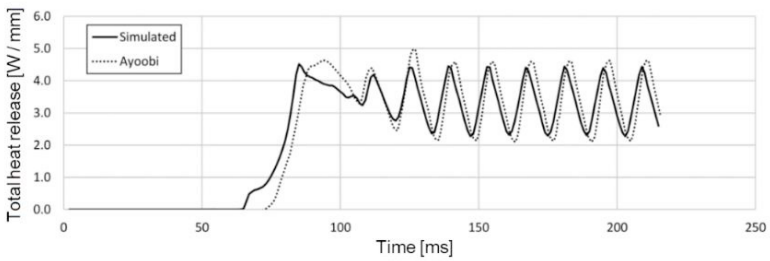

Fig. 6. Heat release fields during ignition and flame stabilization in a 2 by 80 mm-channel for ϕ = 0.7 at: a) 60 ms, b) 70 ms, c) 80 ms, d) 90 ms. A symmetric flame stabilizes after initial behaviour. The field maps are scaled from zero (grey) to 3 W/mm^3 (black).

The increasing of the channel height from 2 to 5 mm drastically changes the flame dynamics, as shown in Fig. 6 for ϕ = 0.53, illustrating the total heat release as a function of time. The flame continues to be ignited further downstream where the wall temperature is higher, and after an initial total heat release peak, the flame loses its symmetry oscillating back and forth. One end advances in the combustor while the other is receding, originating variations of total heat release, Figure 6. In the steady-state frequency, the deviation errors obtained for the maximum value and its location of total heat release were about 2% and 1%, respectively. However, the differences between the present predictions, with those obtained by Ayoobi, are due to the lower resolution grid, which is practically three times less refined, according to [7].

3.2. Co-flow diffusion flame with H_2/N_2 mixture

The effect of the porous media inside of the burner for co-flow diffusion flame with H_2/N_2 mixture at micro and meso-scale, on the emission of pollutant gases is investigated numerically in three phases, according the sequence of Table 1. Fig. 7 (a) shows the map of NO_x mass flow rate for different thermal boundary conditions of the porous surfaces for the tests (a.0) and (a.1); there are practically no differences between the different thermal boundary conditions applied to the porous surface. The porous inserted does not influence much the NO_x formation, as the flow goes around it.

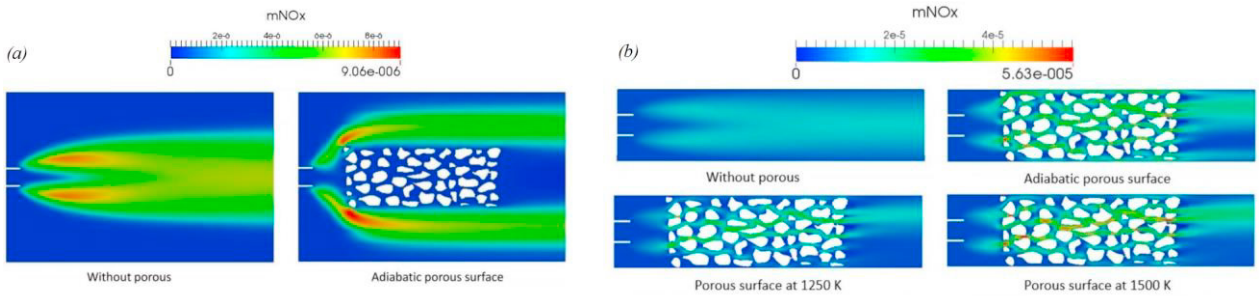

Fig. 7. Map of mass flow rate of NO_x, co-flow flames for different cases: (a) tests (a) and (b) tests (b).

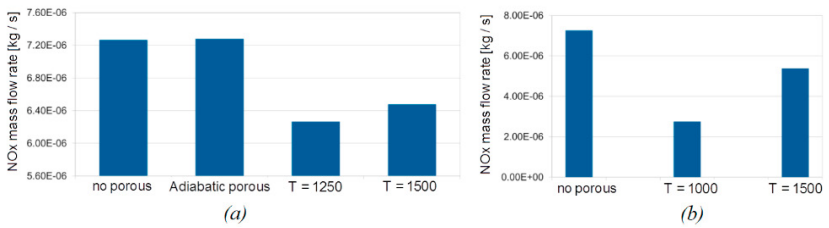

Fig. 8. Mass flow rate of NO_x for different thermal BC at the porous surface, at the outlet of the combustor, of H_2/N_2 co-flow flames for: (a) tests (b.0, b.1, b.3 and b.4) and (b) tests (c.0, b.2 and b.4)

Relatively to tests (b), represented in Fig. 7 (b), there are some differences. The combustion flow already propagates through the porous media and is influenced by the boundary conditions. The tests without porous and with adiabatic porous surface produce more NO_x, since the temperature is high. The source for NO_x is the thermal NO_x. Its formation rate depends on the temperature and residence time of N_2 found in the combustion air at that temperature. When a temperature lower than the flame temperature is imposed to the porous surface, the thermal NO_x is reduced, as it can be observed in the comparison of the results for the adiabatic wall and T = 1250 K, presented in Figure 8 (a). Increasing the porous wall temperature up to 1500 K, increases the thermal NO_x formation, as expected.

Relatively to tests (c), shown in Fig. 8 (b) and Fig. 9, the same conclusions can be taken as for tests (b). The tests without porous and with adiabatic porous surface produce more NO_x, whereas the lower temperature profile imposed

to the porous surface produces a lower value of NO_x. Furthermore, the effect of the porous compression from tests (b) to (c) made the combustion flow go through the smaller porous holes, contacting closer to the porous surface, resulting in less production of NO_x. This means the combustion flow will have higher velocities going through the smaller porous region, therefore the residence time is lower, which also results in lower NO_x formation.

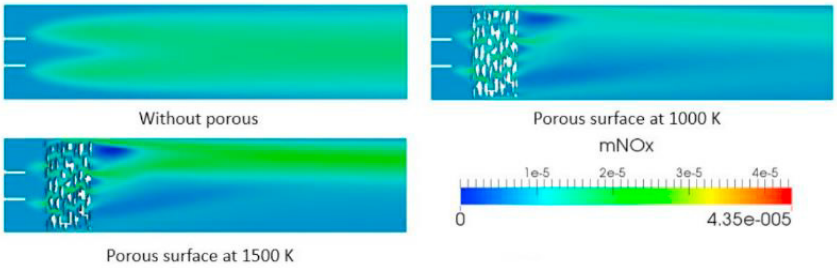

Fig. 9. Map of mass flow rate of NO_x co-flow flames for the cases (c).

4. Conclusions

A numerical study is performed in order to elucidate the emission of NO_x, formed in the co-flow diffusion flame with H_2/N_2 mixture at micro and meso-scale, with a porous media inside the burner. Initially, a numerical study of the dynamics of a CH_4/air premixed flame in a narrow 2D channel, with different conditions, was made, to recreate the Ayoobi numerical results to validate the numerical code. The predictions were able to capture the stationary and oscillating flames for the different conditions, with good agreement with the Ayoobi results. Reducing the size of the porous media, and consequently the porous holes that the combustion flow has to go through, results in higher velocities of the flow and therefore lower residence times, leading to lower NO_x formation. Furthermore, the decrease of the temperature, imposed at the porous surface also decreased the NO_x formation.

Acknowledgements

Financial support provided by FAPESP - Fundação de Amparo à Pesquisa do Estado de São Paulo through Project Nº 2015/26842-3 is gratefully acknowledged by P. R. Resende.

References

[1] Ju Y and Maruta K. Microscale combustion: Technology development and fundamental research. Progress in Energy and Combustion Science 2011; 37: 669-715.
[2] Aikun T, Jianfeng P, Xia S and Hong X. Numerical simulation study of premixed Hydrogen-Oxygen combustion process in micro-scale rectangular channel. In: International Conference on Computer Distributed Control and Intelligent Environmental Monitoring: IEEE; 2011.
[3] Li J, Chou SK, Li ZW and Yang WM. A comparative study of H2-air premixed flame in micro combustors with different physical and boundary conditions. Combustion Theory and Modelling 2008; 12 (2): 325-347.
[4] Chen C-H and Ronney PD. Scale and geometry effects on heat-recirculating combustors. Combustion Theory and Modelling 2013; 17 (5): 888–905.
[5] Li J, Wang Y, Shi J and Liu X. Dynamic behaviors of premixed hydrogen–air flames in a planar micro-combustor filled with porous medium. Fuel 2015; 145: 70–78.
[6] Cuoci A, Frassoldati A, Faravelli T and Ranzi E. A computational tool for the detailed kinetic modeling of laminar flames: Application to C2H4/CH4 coflow flames. Combustion and Flame 2013; 160: 870-886.
[7] Ayoobi M. Chemical structures and dynamics in laminar flame propagation [PhD Thesis]. Louisiana State University; 2015.
[8] Hall J. The radiative source term for plane-parallel layers of reacting combustion gases. Journal of Quantitative Spectroscopy and Radiative Transfer 1993; 49 (5): 517-523.
[9] Coffee TP and Heimerl JM. Transport algorithms for premixed, laminar steady-state flames. Combustion and Flame 1981; 43: 273-289.
[10] Ranzi E, Frassoldati A, Grana R, Cuoci A, Faravelli T, Kelley AP and Law CK. Hierarchical and comparative kinetic modeling of laminar flame speeds of hydrocarbon and oxygenated fuels. Progress in Energy and Combustion Science and Technology 2012; 38 (4): 468-501.